Electronic Supplementary Material (ESI) for Green Chemistry.

Electronic Supporting Information

to

Mechanochemical insertion of cobalt into porphyrinoids using $Co_2(CO)_8$ as a cobalt source

Dinusha Damunupola[a], Nivedita Chaudhri[a], Adewole O. Atoyebi[a], and Christian Brückner[a]*

[a]*Department of Chemistry, University of Connecticut, Storrs, CT 06269-3060, U.S.A.*

c.bruckner@uconn.edu

+1 (860) 486-2743

Table of Contents

1. Milling Parameters: Grinding Speed, Time, Vessel Size, and Vessel Material

Table S1. Effects of grinding speed, time, and vessel size/material on the outcome of the mechanochemical insertion of cobalt into **OEP** using $Co_2(CO)_8$ in a planetary mill using the parameters indicated.

Reaction	Milling speed	Yield[a] after milling time
$Co_2(CO)_8$ (34 mg, 2.5 equiv), basic Al_2O_3 (0.5 g), LiOH (50 mg), **OEP** (20 mg, 1 equiv) → milling speed, time, 50 mL agate vessel → **[OEP]Co** (yield after x time)	400 rpm	30%, 70 min
	600 rpm	40%, 50 min
	800 rpm	95%, 35 min
Reaction	**Vessel size & material**	**Yield[a] after milling time**
$Co_2(CO)_8$ (34 mg, 2.5 equiv), basic Al_2O_3 (0.5 g), LiOH (50 mg), **OEP** (20 mg), 1 equiv) → 800 rpm, time, vessel size & material → **[OEP]Co** (yield after x time)	12.5 mL, agate	95%, 45 min
	44 mL, zirconia	55%, 45 min
	50 mL, agate	95%, 35 min

Notes:

[a] Isolated yields.

The zirconia vessels used were factory-new with very smooth surfaces, whereas the surfaces of the agate vessels were much rougher; also, the zirconia balls used were significantly smaller than the agate counterparts. The combination of these factors likely contributed to the lower metal insertion efficiency of the reaction studied.

The choice of grinding aid and the added base are the optimized conditions discussed in the manuscript.

2. [Octaethylporphyrinato]cobalt(II) ([OEP]Co)

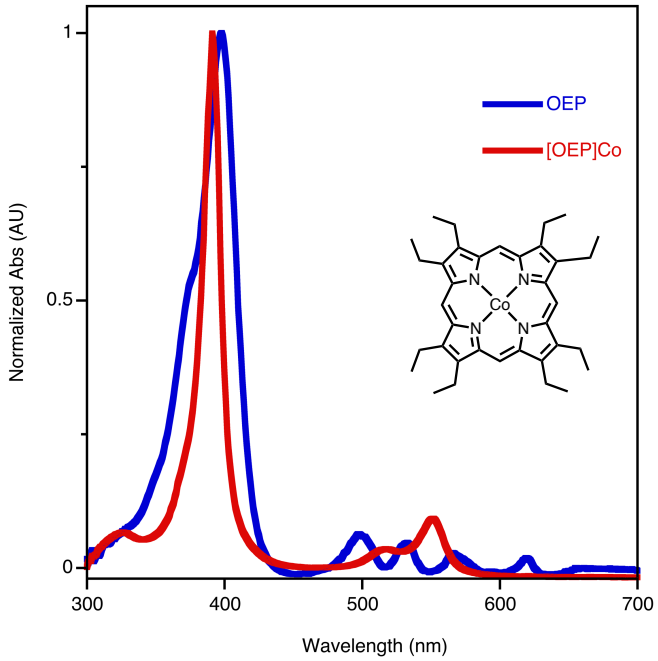

Figure S1. UV-vis spectrum (CH_2Cl_2) of **[(OEP]Co** in comparison to that of the corresponding free base **OEP**. **[OEP]Co** is literature-known.[1]

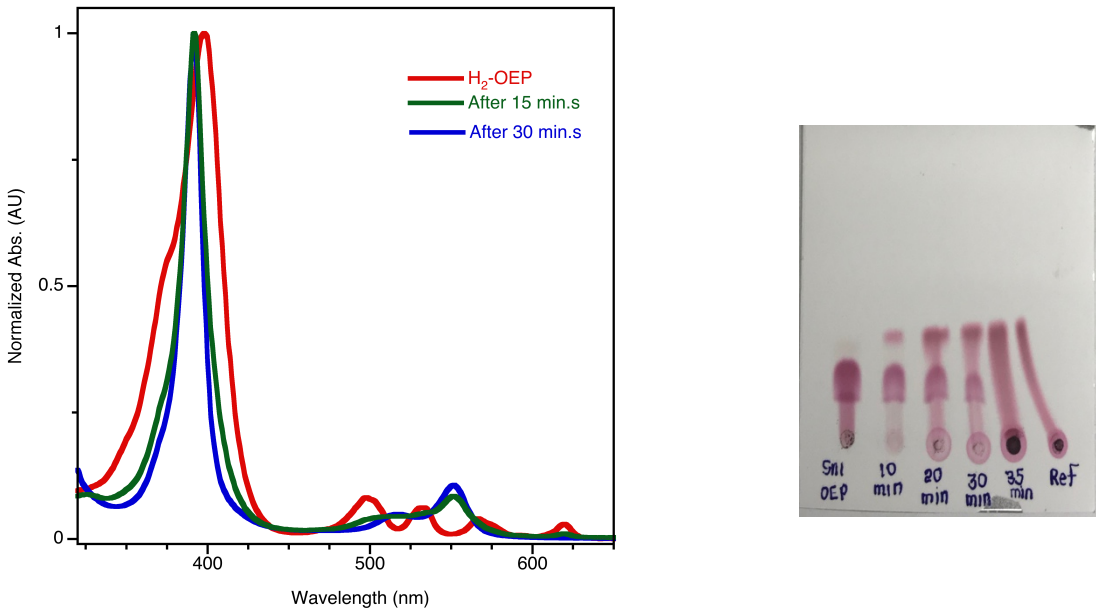

Figure S2. Left: UV-vis spectrum (CH_2Cl_2) of **[OEP]Co** in comparison to that of the corresponding free base **OEP** over the reaction time. Right: representative TLC image used to judge the progress of the metal insertion reaction (silica-ethyl acetate:hexanes:MeOH-55:40:5).

3. [2-Oxooctaethylchlorinato]cobalt(II) ([2-oxo-OEP]Co)

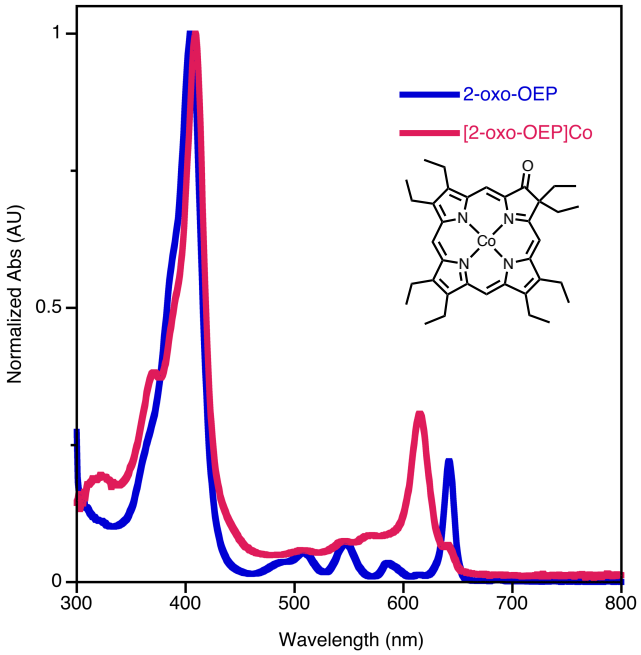

Figure S3. UV-vis spectrum (CH_2Cl_2) of **[2-oxo-OEP]Co** in comparison to that of the corresponding free base **2-oxo-OEP**. **[2-oxo-OEP]Co** reported here firstly.

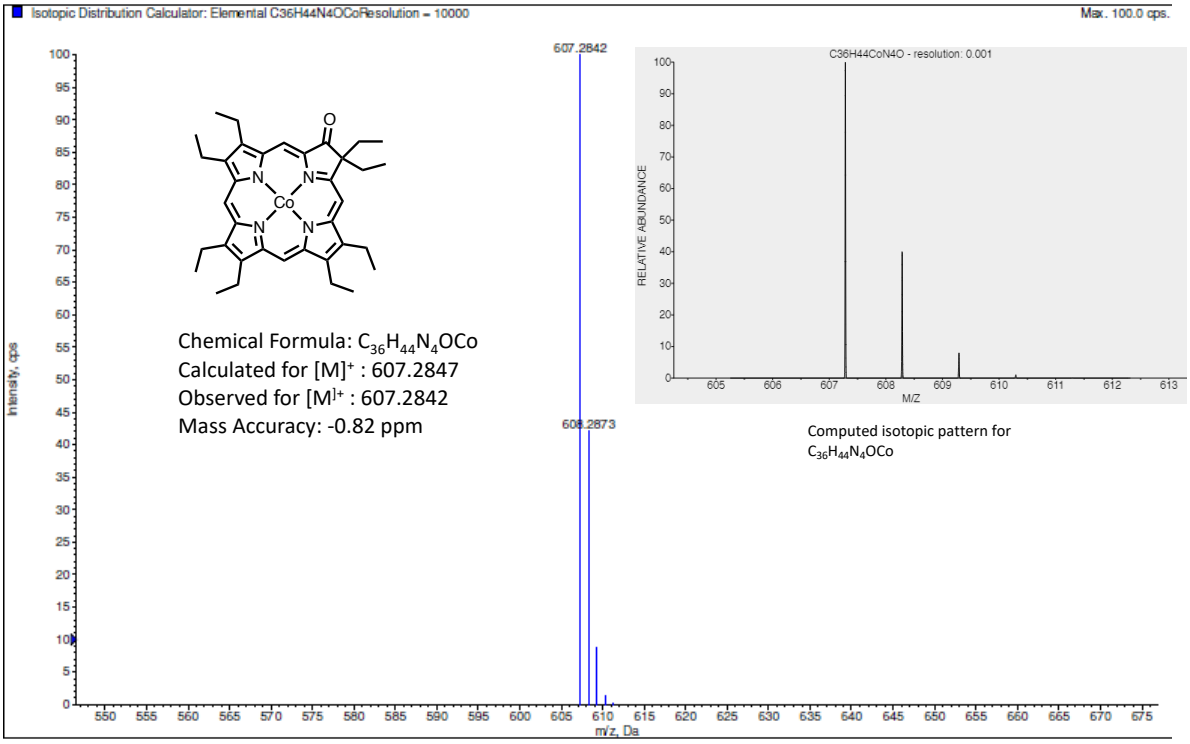

Figure S4. ESI+ HR-MS (100% CH_3CN, TOF) of **[2-oxo-OEP]Co**.

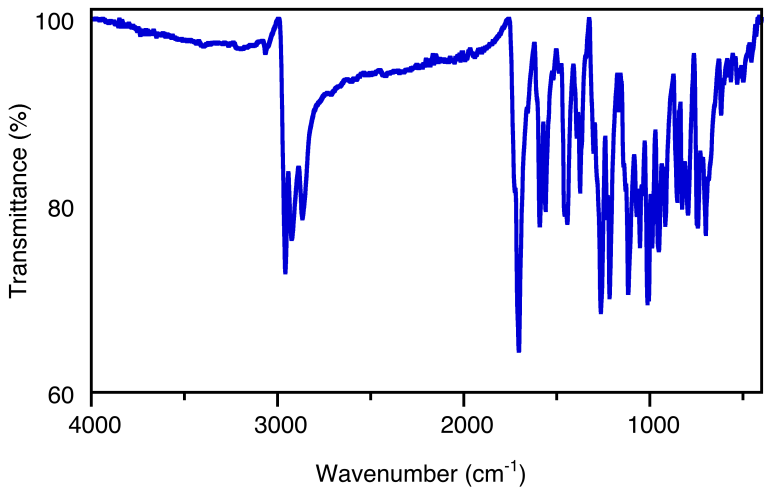

Figure S5: FT-IR spectrum (neat, diamond ATR) of **[2-oxo-OEP]Co**.

4. [2,7-Dioxooctaethylisobacteriochlorinato]cobalt(II) ([2,7-dioxo-OEP]Co)

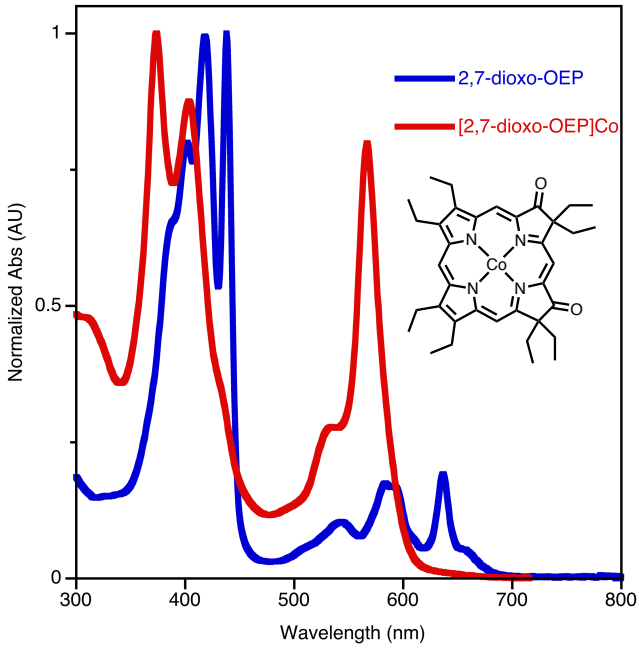

Figure S6. UV-vis spectrum (CH_2Cl_2) of **[2,7-dioxo-OEP]Co** in comparison to that of the corresponding free base **2,7-dioxo-OEP**. **[2,7-dioxo-OEP]Co** is reported here firstly.

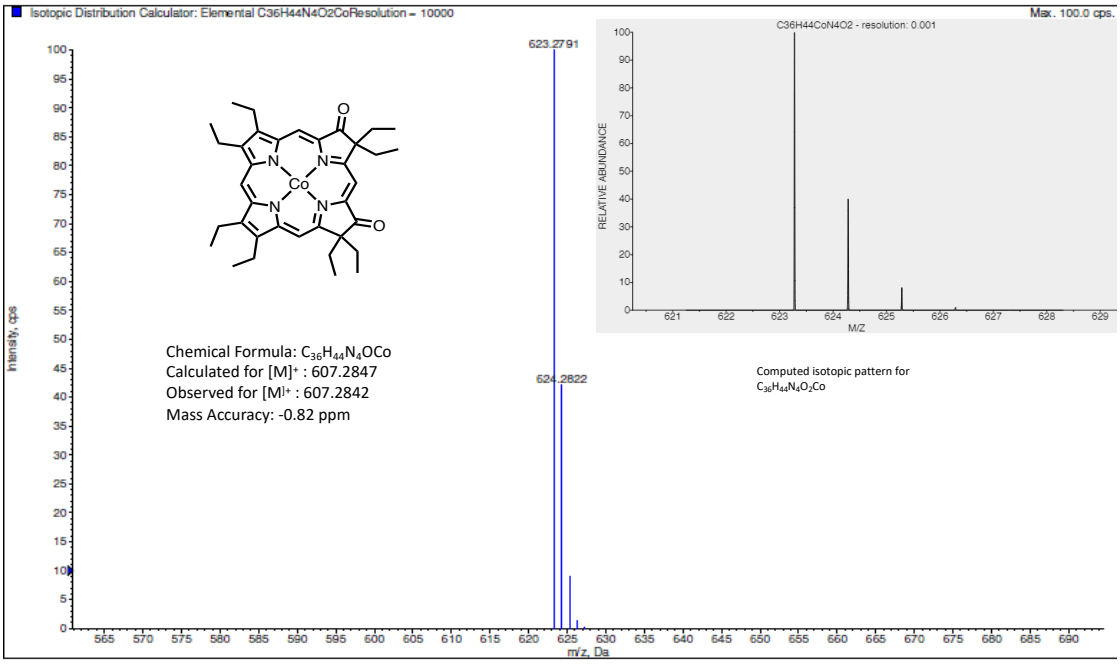

Figure S7. ESI+ HR-MS (100% CH_3CN, TOF) of **[2,7-dioxo-OEP]Co**.

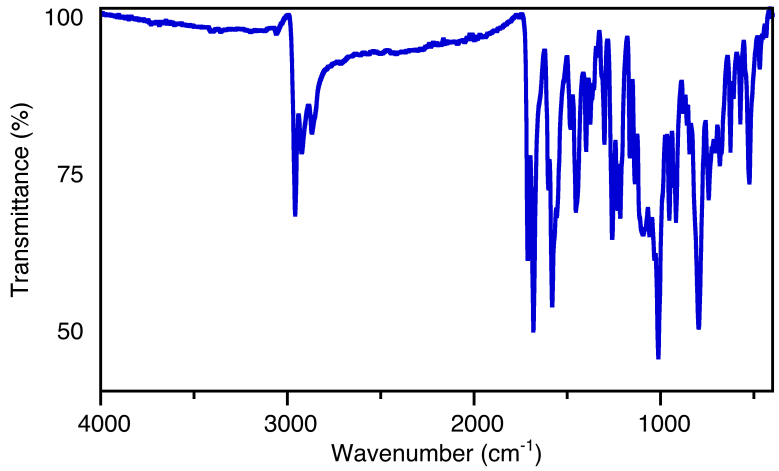

Figure S8: FT-IR spectrum (neat, diamond ATR) of **[2,7-dioxo-OEP]Co**.

5. [2,12-Dioxooctaethylbacteriochlorinato]cobalt(II) ([2,12-dioxo-OEP]Co)

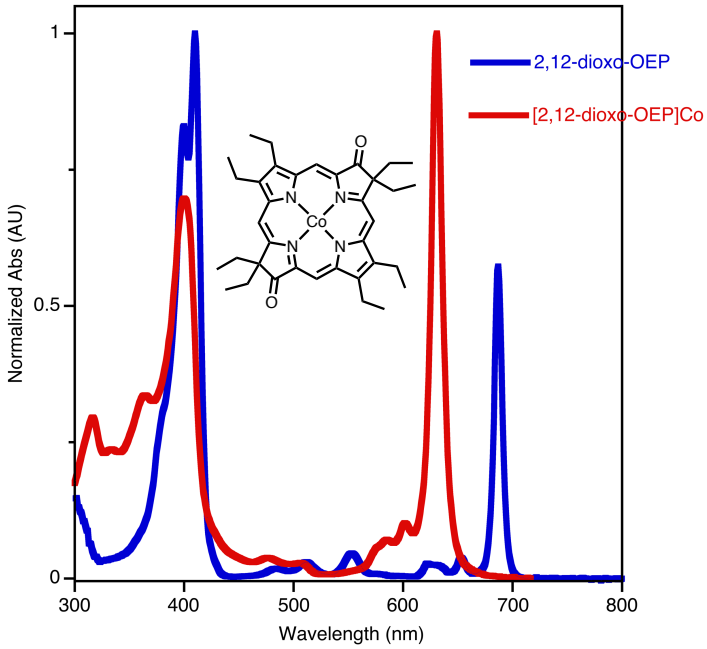

Figure S9. UV-vis spectrum (CH_2Cl_2) of **[2,12-dioxo-OEP]Co** in comparison to that of the corresponding free base **2,12-dioxo-OEP**. **[2,12-dioxo-OEP]Co** is reported here firstly.

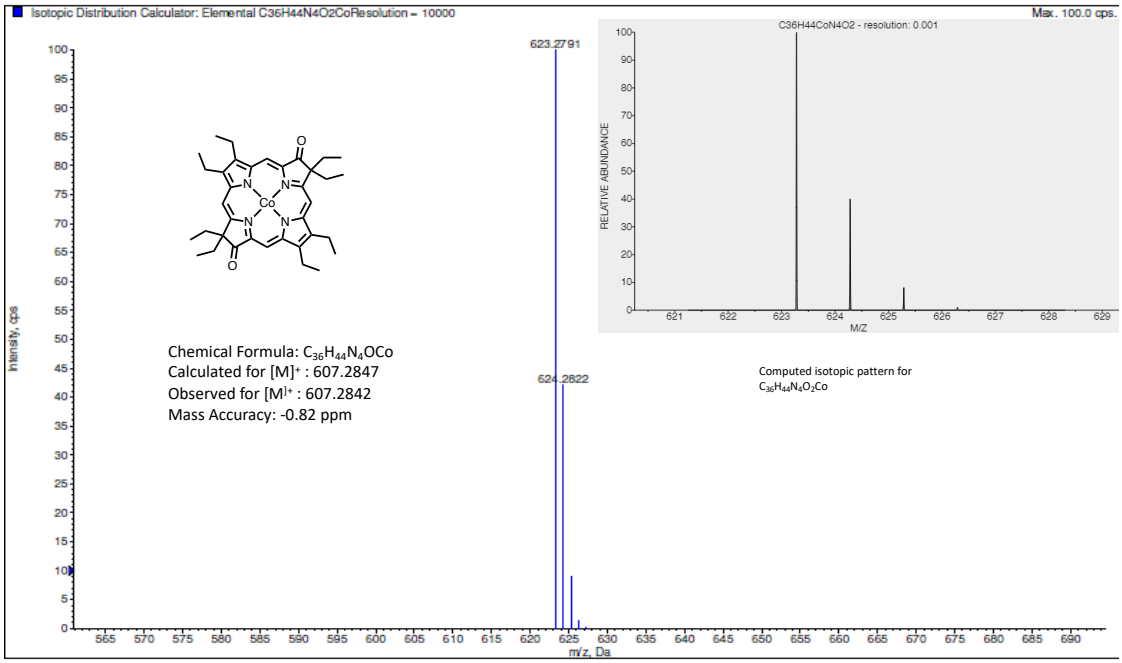

Figure S10. ESI+ HR-MS (100% CH_3CN, TOF) of **[2,12-dioxo-OEP]Co**.

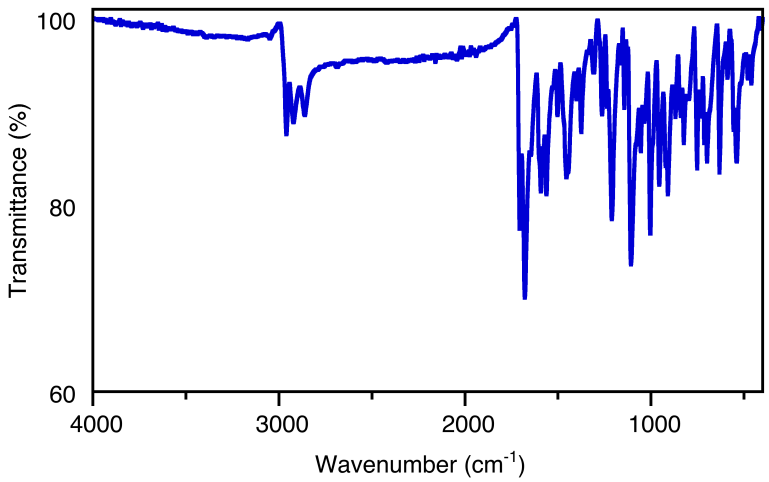

Figure S11: FT-IR spectrum (neat, diamond ATR) of **[2,12-dioxo-OEP]Co**

6. [2,7,18-Trioxo-octaethylpyrrocorphyrinato]cobalt(II) ([2,7,18-trioxo-OEP]Co)

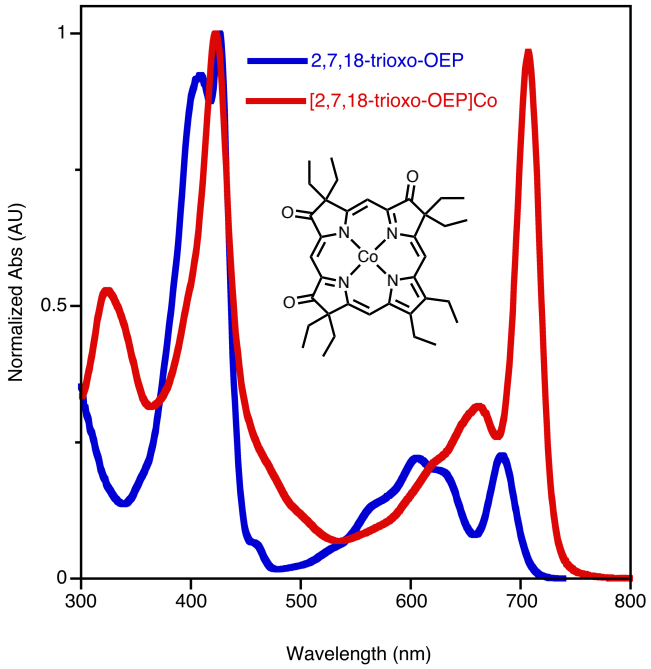

Figure S12. UV-vis spectrum (CH_2Cl_2) of **[2,7,18-trioxo-OEP]Co** in comparison to that of the corresponding free base **2,12,18-trioxo-OEP**. **[2,7,18-dioxo-OEP]Co** is reported here firstly.

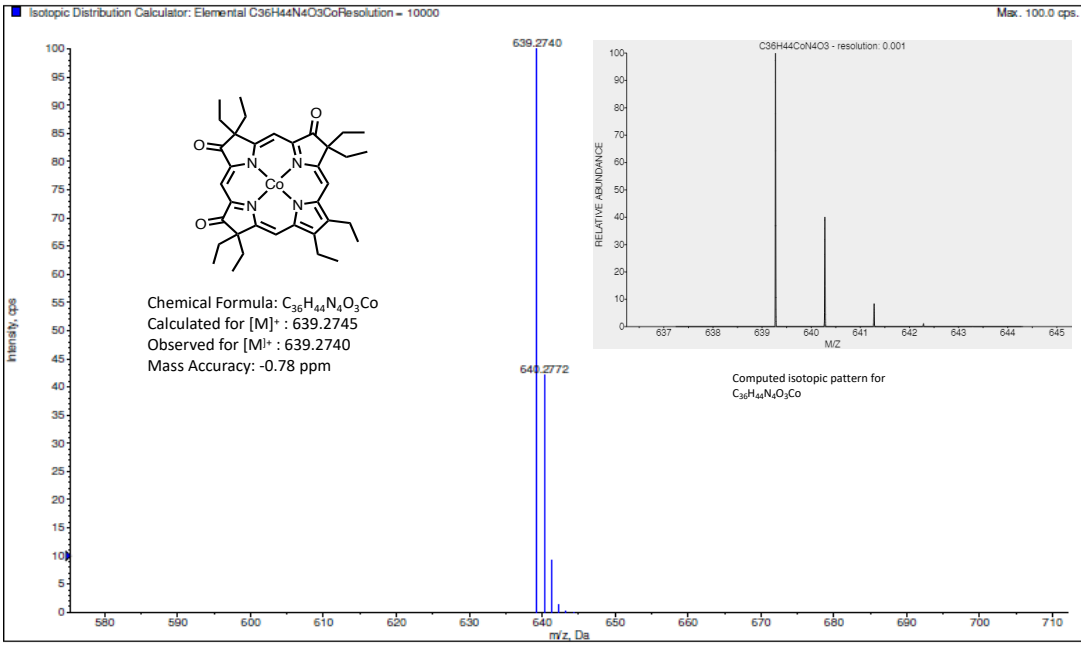

Figure S13. ESI+ HR-MS (100% CH_3CN, TOF) of **[2,7,12-trioxo-OEP]Co**.

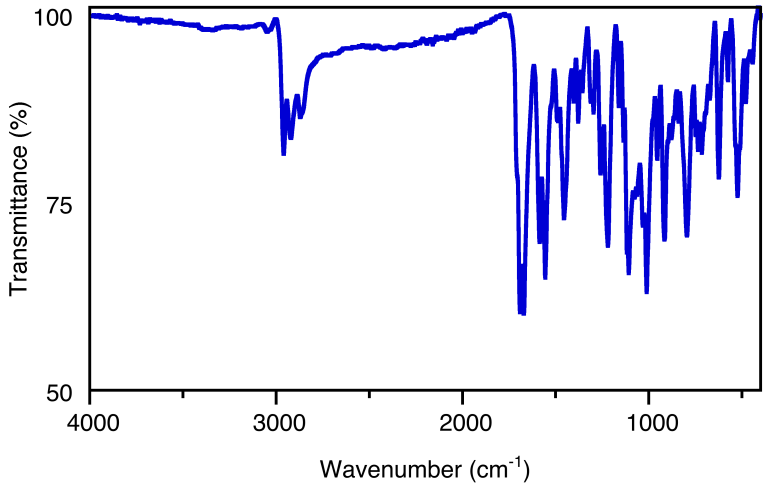

Figure S14: FT-IR spectrum (neat, diamond ATR) of **[2,7,18-trioxo-OEP]Co**

7. [*meso*-Tetraphenylporphyrinato]cobalt(II) ([TPP]Co)

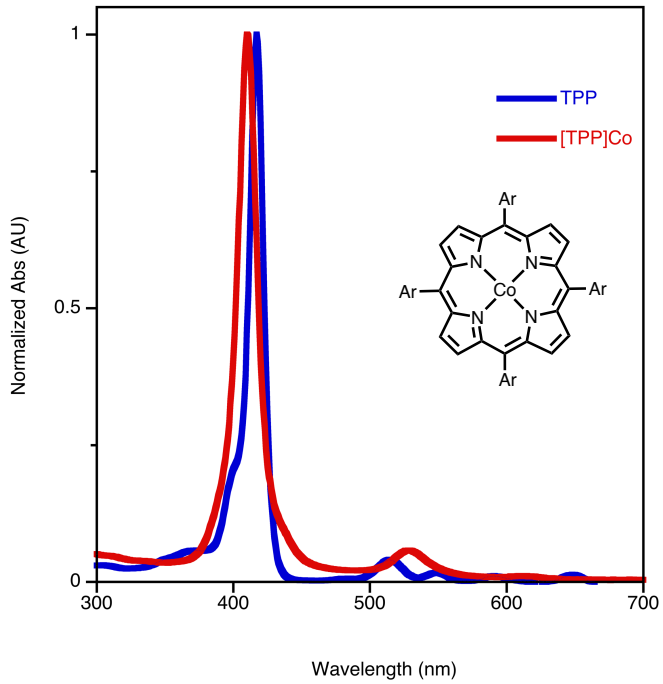

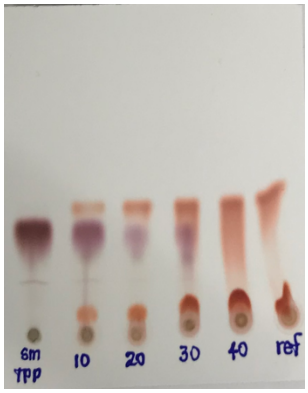

Figure S15. Left: UV-vis spectrum (CH_2Cl_2) of **[TPP]Co** in comparison to that of the corresponding free base **TPP**. Right: representative TLC image used to judge the progress of the metal insertion reaction (silica-ethyl acetate:hexanes-60:40). **[TPP]Co** is literature-known.[1]

8. [*meso*-Tetrakis(pentafluorophenyl)porphyrinato]cobalt(II) ([T^{F}PP]Co)

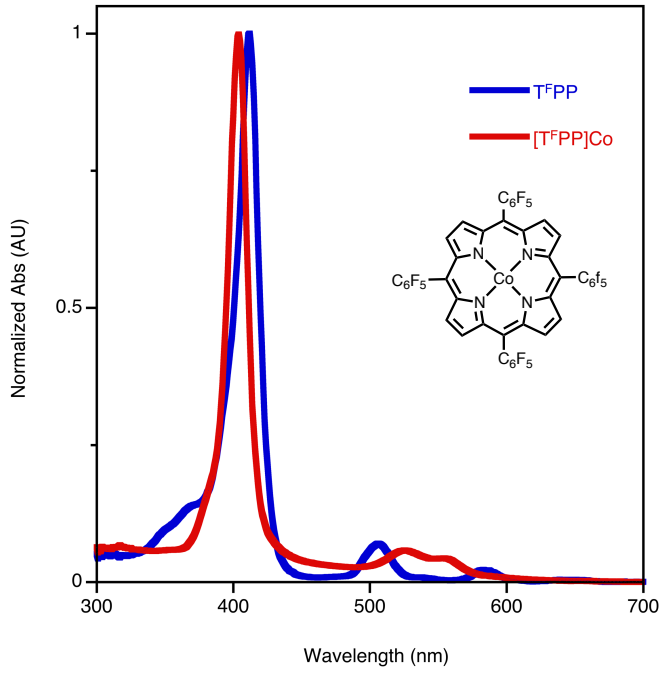

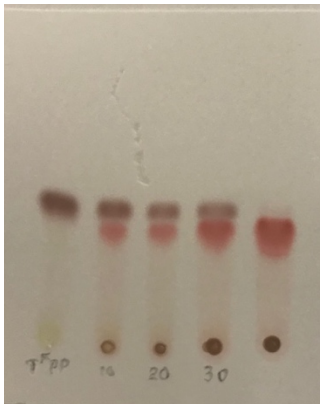

Figure S16. Left: UV-vis spectrum (CH_2Cl_2) of **[T^{F}PP]Co** in comparison to that of the corresponding free base **T^{F}PP**. Right: representative TLC image used to judge the progress of the metal insertion reaction (silica-ethyl acetate:hexanes-70:30). **[T^{F}PP]Co** is literature-known.[2]

9. [*meso*-Tetrakis(4-methoxyphenyl)porphyrinato]cobalt(II) ([T(*p*-OMeP)P]Co)

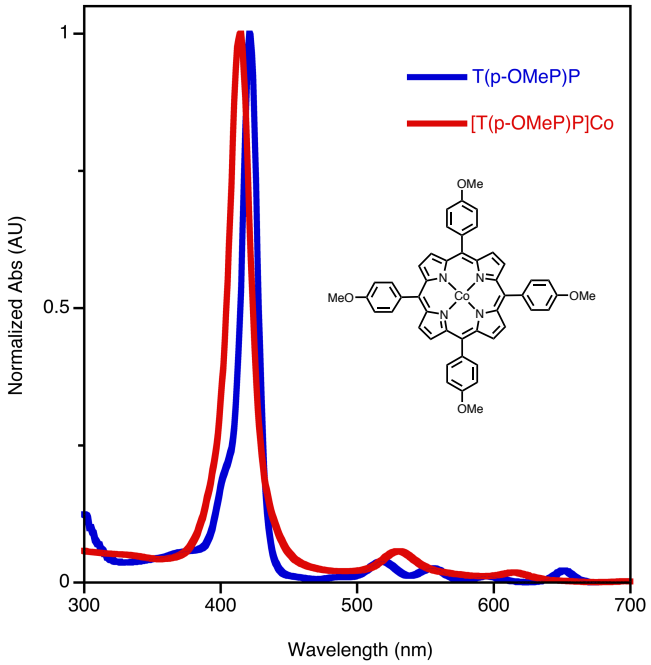

Figure S17. UV-vis spectrum (CH_2Cl_2) of **[T(*p*-OMeP)P]Co** in comparison to that of the corresponding free base **T(*p*-OMeP)P**. **[T(*p*-OMeP)P]Co** is literature-known.[3]

10. [*meso*-Tetrakis(4-chlorophenyl)porphyrinato]cobalt(II) ([T(*p*-ClP)P]Co)

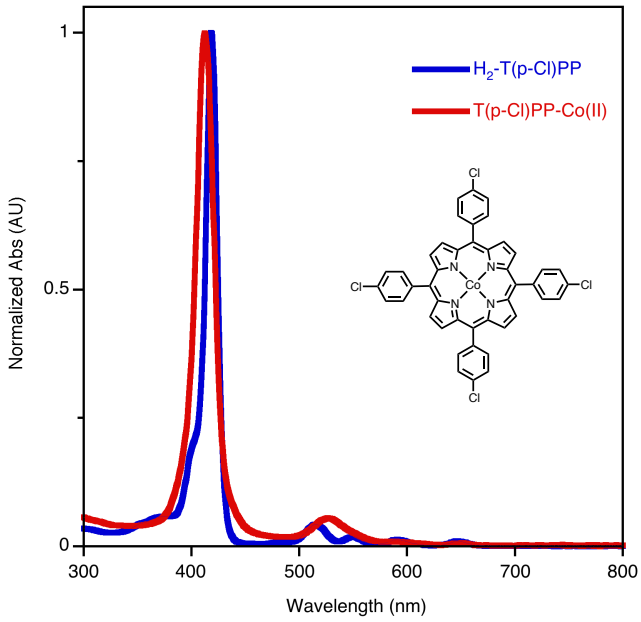

Figure S18. UV-vis spectrum (CH_2Cl_2) of **[T(*p*-ClP)P]Co** in comparison to that of the corresponding free base **T(*p*-ClP)P**.

11. [*meso*-Tetrakis(pentafluorophenyl)lactonato]cobalt(II) ([T^{F}PL]Co)

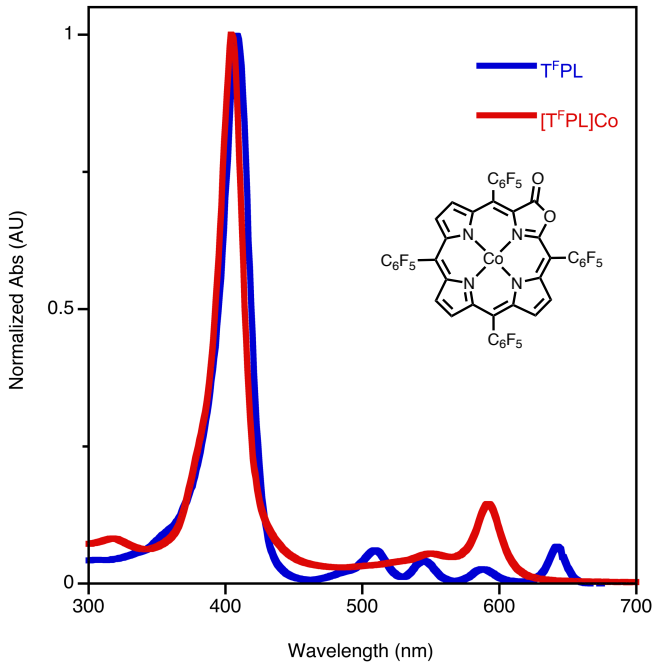

Figure S19. UV-vis spectrum (CH_2Cl_2) of **[T^{F}PL]Co** in comparison to that of the corresponding free base **T^{F}PL**. **[T^{F}PL]Co** reported here firstly.

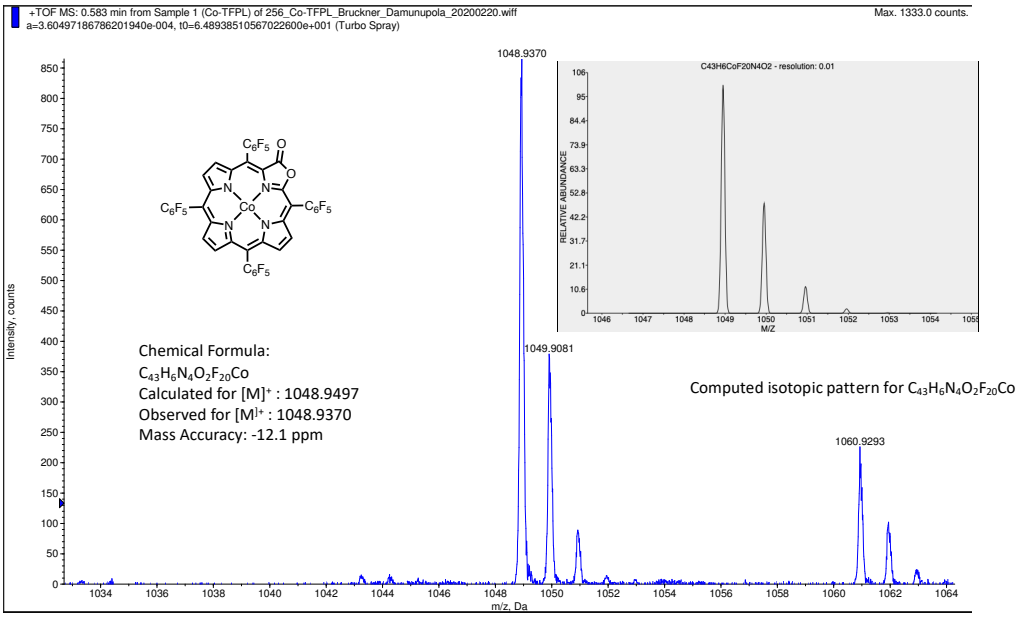

Figure S20. ESI+ HR-MS (100% CH_3CN, TOF) of **[T^{F}PL]Co**.

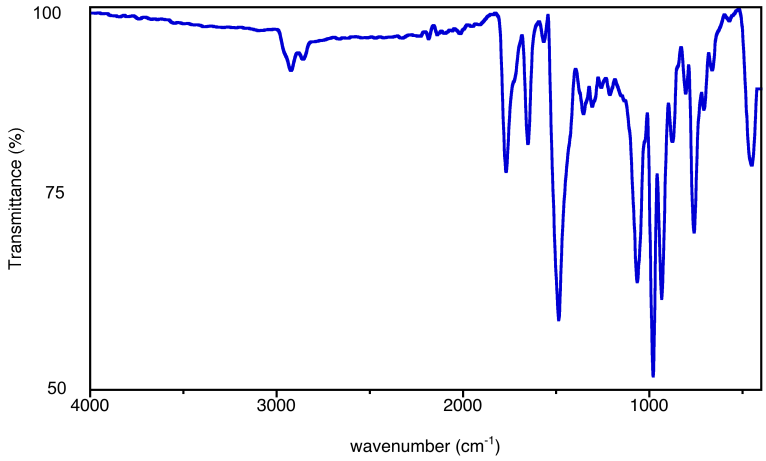

Figure S21. FT-IR spectrum (neat, diamond ATR) of **[T^{F}PL]Co**.

12. [*meso*-Tetrakis(4-*tert*-butyl-phenyl)lactonato]cobalt(II) ([T(*p*-^{t}BuP)L]Co)

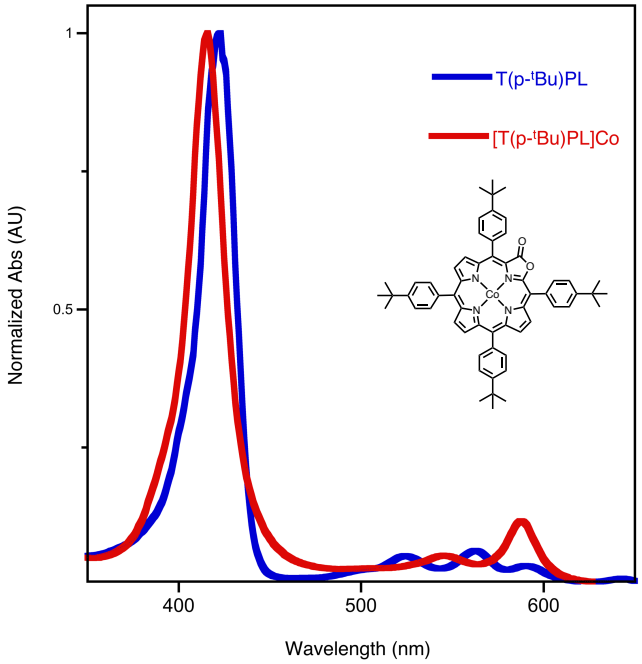

Figure S22. UV-vis spectrum (CH_2Cl_2) of **[T(*p*-^{t}BuP)L]Co** in comparison to that of the corresponding free base **T(*p*-^{t}BuP)L**. **[T(*p*-^{t}BuP)L]Co** reported here firstly.

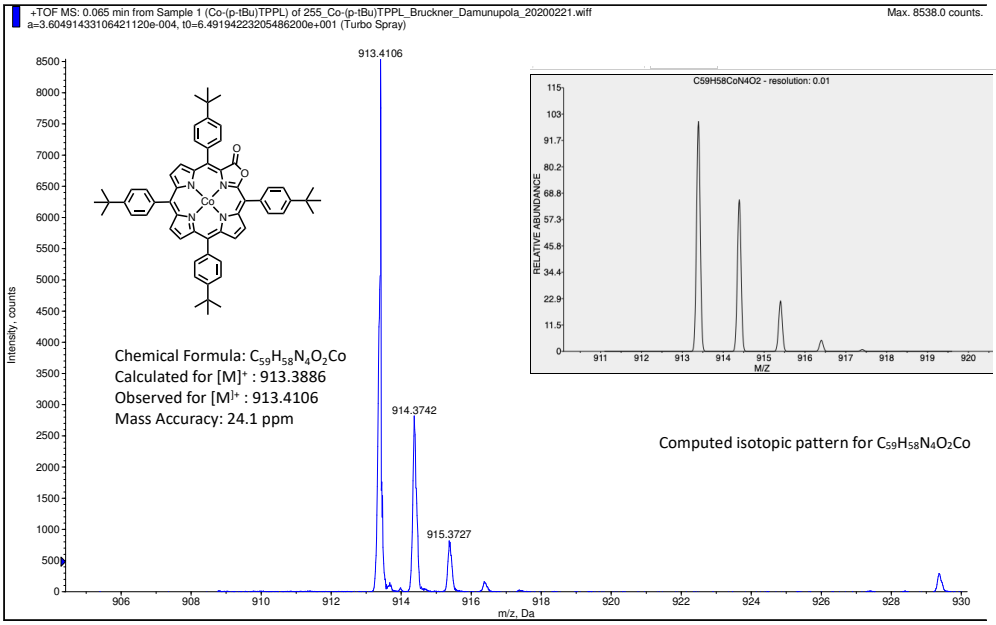

Figure S23. ESI+ HR-MS (100% CH_3CN, TOF) of **[T(*p*-^{t}BuP)L]Co**).

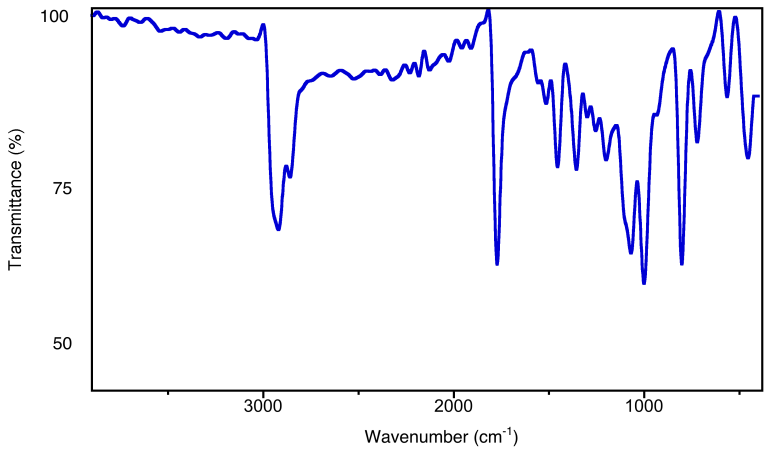

Figure S24. FT-IR spectrum (neat, diamond ATR) of **[T^{F}PL]Co**.

13. [*meso*-Tetra(3-thienyl)porphyrinato]cobalt(II) ([T(³Thie)P]Co)

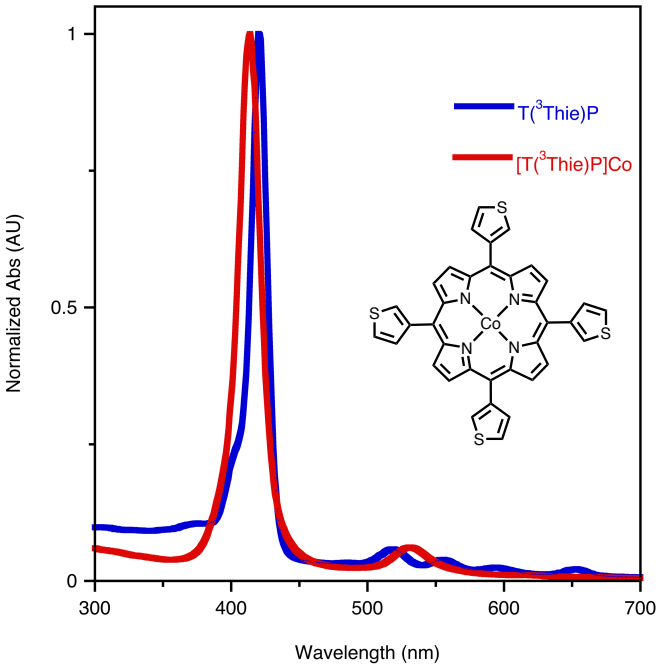

Figure S25. UV-vis spectrum (CH_2Cl_2) of **[T(³Thie)P]Co** in comparison to that of the corresponding free base **T(³Thie)P**. **[T(³Thie)P]Co** is literature-known.[4]

14. [*meso*-Tetrakis(5-methylthienyl)porphyrinato]cobalt(II) ([T(5-Me²Thie)P]Co)

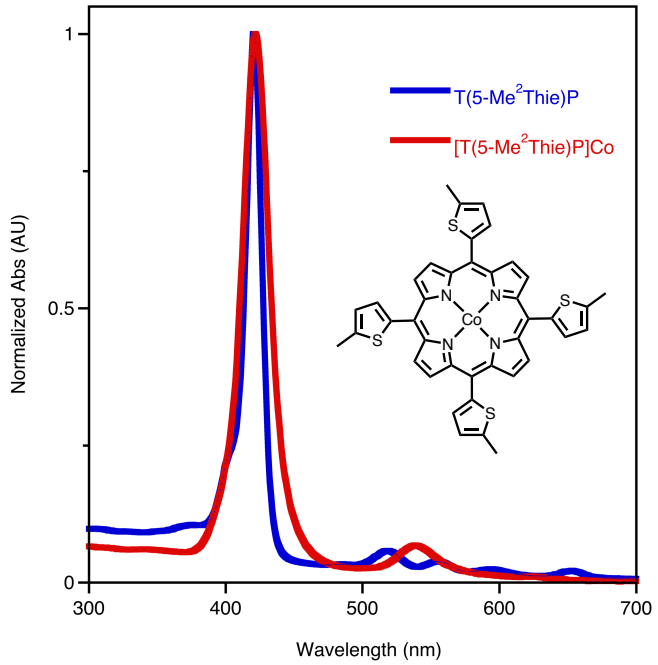

Figure S26. UV-vis spectrum (CH_2Cl_2) of **[T(5-MeT²Thie)P]Co** in comparison to that of the corresponding free base **T(5-Me²Thie)P**. **[T(5-MeT²Thie)P]Co** is literature-known.[4]

15. [*meso*-Tetrakis(pentafluorophenyl)-7,8-*cis*-dihydroxychlorinato]cobalt(II) ([(OH)$_2$T^{F}PC]Co)

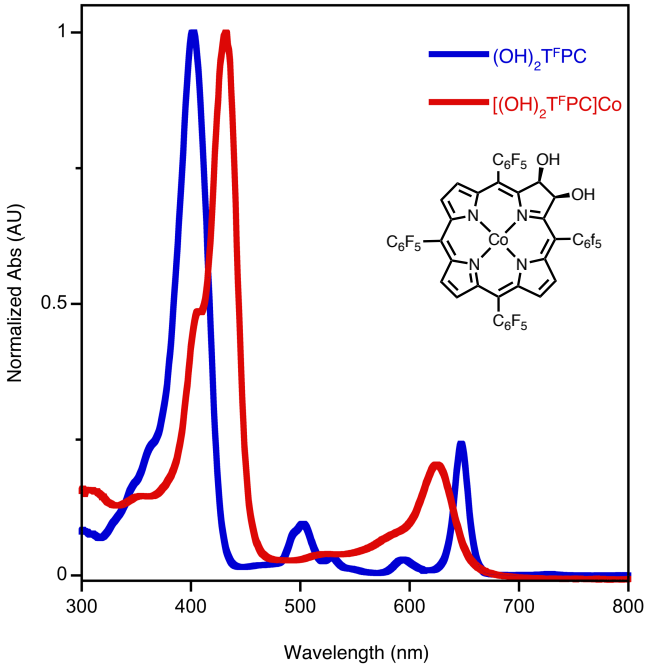

Figure S27. UV-vis spectrum (CH_2Cl_2) of **[(OH)$_2$T^{F}PC]Co** in comparison to that of the corresponding free base **(OH)$_2$T^{F}PC**. **[(OH)$_2$T^{F}PC]Co** reported here firstly.

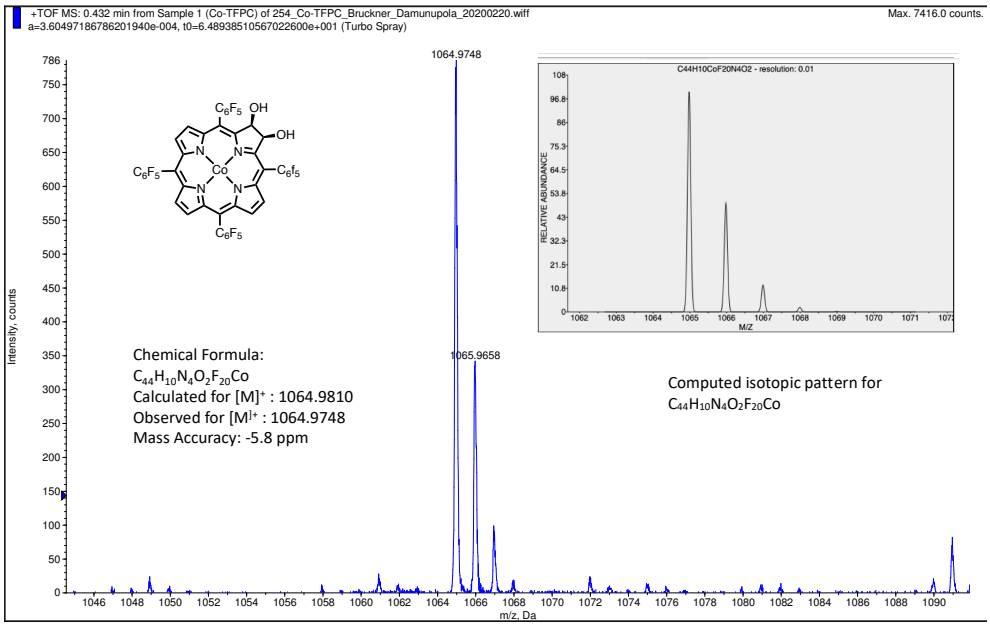

Figure S28. ESI+ HR-MS (100% CH_3CN, TOF) of **[(OH)$_2$T^{F}PC]Co**.

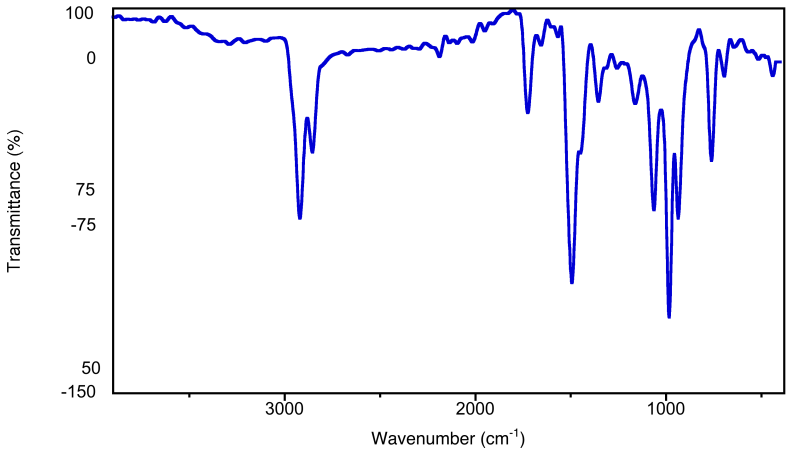

Figure S29. FT-IR spectrum (neat, diamond ATR) of **[(OH)$_2$T^{F}PC]Co**.

16. [*meso*-Tetraphenyl-2,3-*cis*-dihydroxychlorinato]cobalt(II) ([(OH)$_2$TPC]Co)

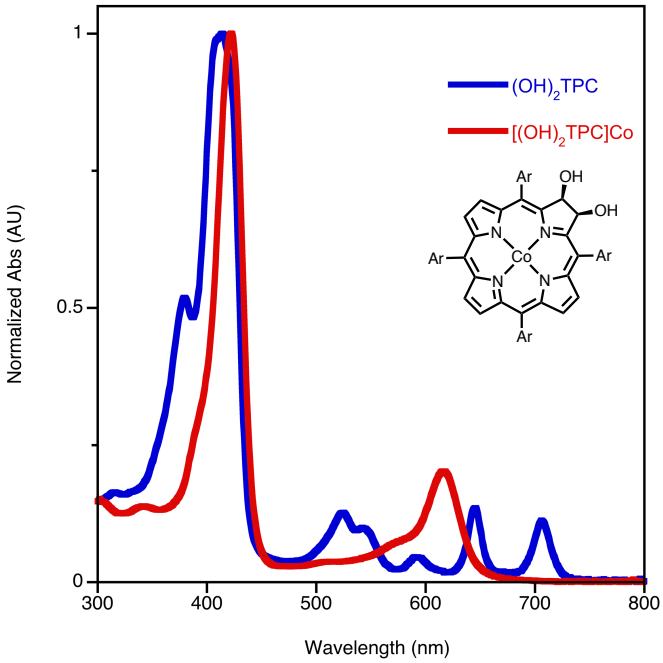

Figure S30. UV-vis spectrum (CH_2Cl_2) of **[(OH)$_2$TPC]Co** in comparison to that of the corresponding free base **(OH)$_2$TPC**. **[(OH)$_2$TPC]Co** is literature-known.[5]

17. [*meso*-Tetraphenyldiethoxymorpholinochlorinato]cobalt(II) ([TPMor]Co)

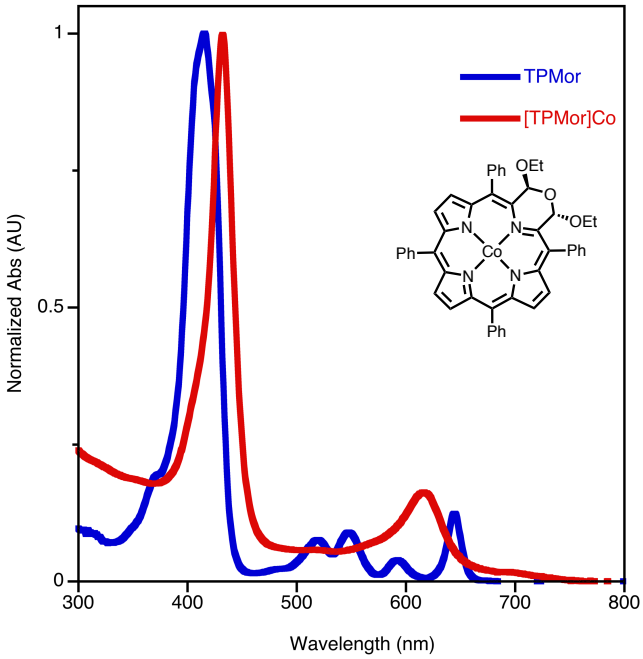

Figure S31. UV-vis spectrum (CH_2Cl_2) of **[TPMor]Co** in comparison to that of the corresponding free base **TPM**. **[TPMor]Co** is literature-known.[6]

18. [5,10-Diphenylindaphyrinato]cobalt(II) ([DPI]Co)

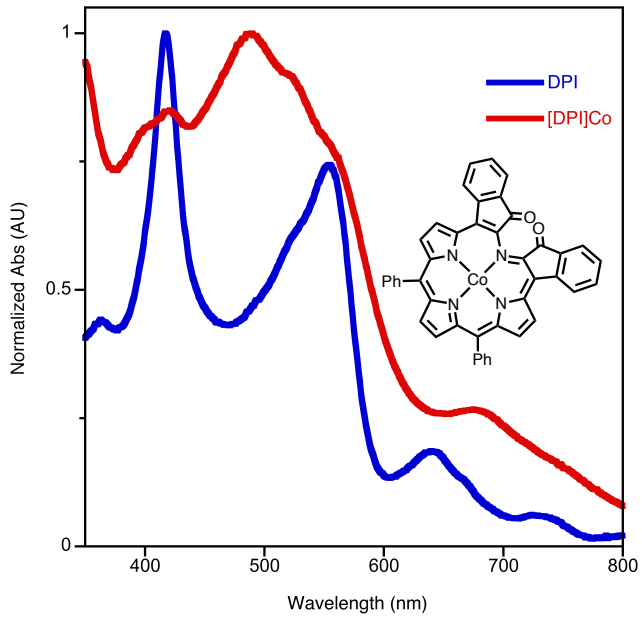

Figure S32. UV-vis spectrum (CH_2Cl_2) of **[DPI]Co** in comparison to that of the corresponding free base **DPI**. **[DPI]Co** is literature-known.[6]

19. [5,10,15-Triphenylcorrolato]cobalt(II) ([TPCor]Co)

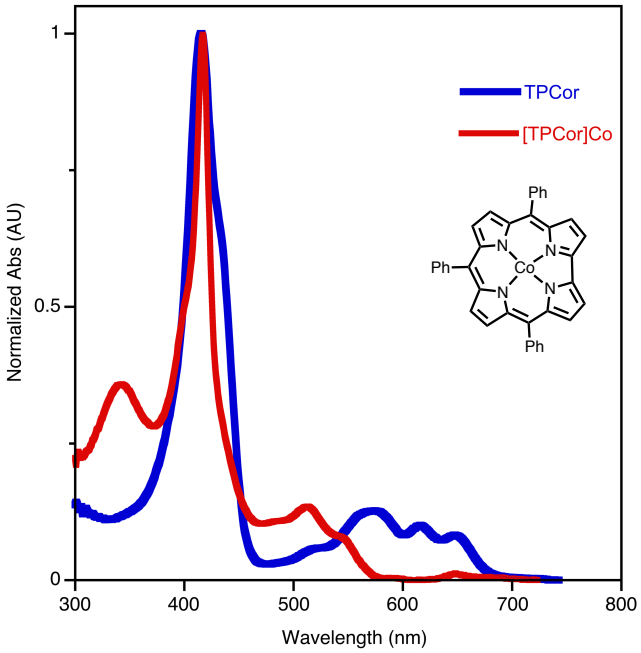

Figure S33. UV-vis spectrum (CH_2Cl_2) of **[TPCor]Co** in comparison to that of the corresponding free base **TPCor**. **[TPCor]Co** is literature-known.[7]

20. References

1. C. D. Tail, D. Holten and M. Gouterman, *J. Am. Chem. Soc.*, 1984, **106**, 6653–6659.
2. D.-X. Zhang, H.-Q. Yuan, H.-H. Wang, A. Ali, W.-H. Wen, A.-N. Xie, S.-Z. Zhan and H.-Y. Liu, *Transition Met. Chem.*, 2017, **42**, 773–782.
3. F. A. Walker, D. Beroiz and K. M. Kadish, *J. Am. Chem. Soc.*, 1976, **98**, 3484–3489.
4. W. Chen, J. Akhigbe, C. Brückner, C. M. Li and Y. Lei, *J. Phys. Chem. C*, 2010, **114**, 8633-8638.
5. E. Mishra, J. L. Worlinsky, T. M. Gilbert, C. Brückner and V. Ryzhov, *J. Am. Soc. Mass Spectrom.*, 2012, **23**, 1135–1147. Erratum (correction of systemic typesetting errors): *J. Am. Soc. Mass. Spectrom.* 2012, **1123**, 1428–1439.
6. E. Mishra, J. L. Worlinsky, C. Brückner and V. Ryzhov, *J. Am. Soc. Mass Spectrom.*, 2014, **25**, 18–29.
7. A. Mahammed, B. Mondal, A. Rana, A. Dey and Z. Gross, *Chem. Commun.*, 2014, **50**, 2725–2727.